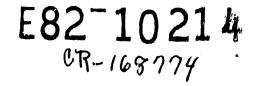
General Disclaimer

One or more of the Following Statements may affect this Document

- This document has been reproduced from the best copy furnished by the organizational source. It is being released in the interest of making available as much information as possible.
- This document may contain data, which exceeds the sheet parameters. It was furnished in this condition by the organizational source and is the best copy available.
- This document may contain tone-on-tone or color graphs, charts and/or pictures, which have been reproduced in black and white.
- This document is paginated as submitted by the original source.
- Portions of this document are not fully legible due to the historical nature of some of the material. However, it is the best reproduction available from the original submission.

Produced by the NASA Center for Aerospace Information (CASI)

"Made available under NASA sponsorship In the interest of carly and wide dissemination of Earth Resources Survey Program information and wildowt hability for any use made thereot."



(E82-10214) TOEGGNATHIC SLOPE CORRECTION N32-23587
 FOR ANALYSIS OF THERMAL INFRAME THERE
 (Geological Survey) 14 p and August AC1
 Unclass
 G3/43 00214

Topographic slope correction for analysis of thermal infrared images

Ъy

Kenneth Watson

U.S. Geological Survey, Box 25046

Denver Federal Center, Denver, CO 80225

(NTIS Report)

Topographic slope correction for analysis of thermal infrared images

by

Kenneth Watson

Abstract

A simple topographic slope correction has been developed using a linearized thermal model and assuming slopes less than about twenty degrees. The correction can be used to analyze individual thermal images or composite products such as temperature difference or thermal inertia. Simple curves are provided for latitudes of 30 and 50 degrees. The form is easily adapted for analysis of HCMM (Heat Capacity Mapping Mission) images using the DMA (Defense Mapping Agency) digital terrain data.

Introduction

Topographic slope effects commonly have been observed on thermal infrared images and are used to deduce geologic structure and morphology (Rowan and others, 1970; Wolfe, 1971; Sabins, 1969; Offield, 1975; Cannon, 1973; Schneider and others, 1979). Some early thermal model studies considered the general nature of slope effects (Watson, 1970; 1971) and it was suggested (Watson and others, 1971) that a simple correction to thermal models could be applied by representing the north-south slope component as an equivalent change in latitude and the east-west component as an equivalent shift in local time.

The initial thermal-inertia study (Pohn and others, 1974), using lowresolution meteorological satellite data, assumed that at that small scale

slopes, and hence topographic effects, were negligible. The first topographically corrected thermal inertia image was constructed from large-scale aircraft data using a lookup table for temperature effects as a function of slope and azimuth derived from a thermal model (Gillespie and Kahle, 1977).

The purpose of this paper is to present an analytical expression for the topographic slope correction to thermal images. This expression will be primarily for the interpretation of data from the HCMM satellite but also applicable to aircraft data under appropriate slope conditions.

Method

A topographic correction term is developed using the linearized thermal model proposed by Watson (1975) and expanded in later studies (Miller and Watson, 1977; Price, 1977; Pratt and Ellyett, 1979; Watson, 1979). The effect of slope is modeled by assuming that it is due solely to the modulation of the incoming direct solar radiation. Second order effects of diffuse and sky radiation, sensible and latent heat, geothermal effects and reradiation from adjacent surfaces have been ignored. These assumptions restrict the model to small slopes (probably less then twenty degrees) and, although generally valid for the 500-m HCMM data, do not apply to large-scale aircraft data acquired in areas of rugged relief.

Let $v(x,t) = v_0(x,t) + v_d(x,t)$ where v is the temperature distribution at a depth x below the Earth's surface and at time t measured from local solar noon, and v(x,t) also satisfies the heat conduction equation in one dimension. v_0 is the temperature for a flat surface and v_d for the additional effect due to an inclined surface of slope d and direction of slope of slope ϕ

(measured counterclockwise from north). The surface boundary condition satisfied by v_d is:

$$-\frac{\partial v_d}{\partial x} = Q_{dir} (\cos z_d - \cos z_o) (1-A) - 4\varepsilon \sigma \overline{v_o}^3 v_d \text{ at } x = 0$$
(1)

and the one dimensional conduction equation is

$$\frac{\partial^2 v_d}{\partial x^2} = \frac{1}{\kappa} \frac{\partial v_d}{\partial t}$$
(2)

where K and κ are the thermal conductivity and diffusivity, A and ε are the surface albedo and emissivity, \overline{v}_0 is the mean surface temperature for the flat surface, σ is the Stefan-Boltzmann constant, Q_{dir} is the amplitude of the incident solar flux (equal to $S_0\tau$ where S_0 is the solar constant and τ the atmospheric transmission factor), z_0 and z_d are the zenith angles of the flat and inclined surfaces, respectively. Using a Fourier series solution (Carslaw and Jaeger, p. 74, 1959) the surface temperature of the inclined surface is:

$$v_{d}(0,t) = Q_{dir} (1-A) (4\varepsilon \sigma^{\frac{3}{7}})^{-1} \sum_{s=0}^{2} \frac{B_{s}h \cos(\omega st - \delta_{s} - \theta_{s})}{\sqrt{(h+W_{s}^{2}) + W_{s}^{2}}}$$
(3)

where the Fourier coefficients B_g and θ_g are derived in Appendix One and the radiation constant h, the wave number W_g and the phase shift δ_g are defined as follows:

$$h = 4\varepsilon\sigma \overline{v_0}^3/K$$

$$W_{g} = \sqrt{\omega g/2\kappa}$$

$$\delta_{g} = \tan^{-1}(W_{g}/(h+W_{g})) \qquad (Watson, 1979).$$

Now because $W_g/h>1$ and $B_k = 0$ for $k = 3, 5, \dots$ then $\delta_g = \pi/4$ and

$$v_{d}(0,t) \approx Q_{dir} (1-A) (4\epsilon g \overline{v_{0}}^{3})^{-1} \left\{ B + \frac{B_{1} \cos (\omega t - \theta_{1} - \pi/4)}{\sqrt{2} (W_{1}/h)} + \sum_{r=1}^{\infty} \frac{B_{2r} \cos (2r\omega t - \theta_{2r} - \pi/4)}{\sqrt{2} (W_{2r}/h)} \right\}$$

Now $W_{2r}/h = \sqrt{2r} (W_1/h)$

where
$$W_1/h = P \sqrt{\omega/2} / (4\varepsilon \sigma v_0^3)$$

and
$$\theta_k = \tan^{-1}(k \tan \phi / \sin \lambda)$$

Therefore, $v_d(0,t) \simeq Q_{dir} (1-A)d (4\varepsilon \sigma v_0^3)^{-1} \left\{ -\frac{\cos \phi \sin \lambda}{\pi} \right\}$

+ (h/W₁) [
$$\frac{\sqrt{\sin \phi + \cos \phi \sin \lambda}}{2\sqrt{2}} \cos (\omega t + \tan^{-1}(\tan \phi/\sin \lambda) - \pi/4)$$

+ $\sum_{r=1}^{\infty} (-1)^{r+1} \frac{\sqrt{(2r \sin \phi)^2 + (\sin \lambda \cos \phi)^2}}{\pi [(2r)^2 - 1] \sqrt{r}}$
• $\cos (2r\omega t + \tan^{-1}(2r \tan \phi/\sin \lambda) - \pi/4)] \}$

Introduce

$$\begin{aligned} \mathbf{v_d}^{\mathrm{DAY}} &= \mathbf{v_d}(0,0) \\ \mathbf{v_d}^{\mathrm{NITE}} &= \mathbf{v_d}(0,T/2) \end{aligned}$$

and $\Delta \mathbf{v_d} &= \mathbf{v_d}(0,0) - \mathbf{v_d}(0,T/2) \\ \text{Then } \mathbf{v_d}^{\mathrm{DAY}} &= \mathbf{Q_{dir}}(1-\mathbf{A}) \ \mathbf{d} \ (4\varepsilon\sigma\overline{\mathbf{v_o}}^3)^{-1} - \cos\phi \ \sin\lambda/\pi \end{aligned}$
 $+ (h/W_1) \left[\frac{\cos\phi \ \sin\lambda + \sin\phi}{4} + \sum_{r=1}^{\infty} \frac{(-1)^{r+1} (2r \ \sin\phi + \sin\lambda \ \cos\phi)}{\pi \ \sqrt{2r}} \right] \right\} \\ \mathbf{v_d}^{\mathrm{NITE}} &= \mathbf{Q_{dir}} \ (1-\mathbf{A}) \ \mathbf{d} \ (4\varepsilon\sigma\overline{\mathbf{v_o}}^3)^{-1} \ \left\{ -\cos\phi \ \sin\lambda/\pi \ + (h/W_1) \ \left[-\frac{\cos\phi \ \sin\lambda + \sin\phi}{4} + \sum_{r=1}^{\infty} \frac{(-1)^{r+1} (2r \ \sin\phi + \sin\lambda \ \cos\phi)}{\pi \ \sqrt{2r}} \right] \right\} \\ (h/W_1) \ \left[-\frac{\cos\phi \ \sin\lambda + \sin\phi}{4} + \sum_{r=1}^{\infty} \frac{(-1)^{r+1} (2r \ \sin\phi + \sin\lambda \ \cos\phi)}{\pi \ \sqrt{2r}} \right] \right\} \\ \text{and } \Delta \mathbf{v_d} &= \mathbf{Q_{dir}} (1-\mathbf{A}) \ \mathbf{d} \ (4\varepsilon\sigma\overline{\mathbf{v_o}}^3)^{-1} \ \left[(h/W_1) \ \left\{ \frac{\cos\phi \ \sin\lambda + \sin\phi}{2} \right\} \right] \end{aligned}$

The temperature-difference effect is proportional to slope and the azimuth variation, which is the term in brackets ([]), and is plotted for the day, night, and temperature difference in Figure 1 using an assumed value of (h/W_1) . The amplitudes of the three expressions are roughly similar, and this shows that the temperature-difference expression does not provide any reduction of the topographic slope effect as an improvement over the individual day and night images. There are orientation effects, however, that can cause the topographic effect to be more pronounced in our image. An HCMM test site in Cabeza Prieta, Ariz. (latitude 30°) has a general NW-SE topographic grain-corresponding to $\phi = 135^{\circ}$ and 315° . At these azimuths, the topographic effect should be least in the temperature-difference image (and hence thermal inertia which is derived from it) and greatest in the daytime thermal image. Conclusion

The general expression given for the topographic correction, equation 5, can be easily modified for other data acquisition times and latitudes. An expression for Q_{dir} can be obtained for clear sky conditions (Hummer-Miller, 1981) and the value of W_1/h computed as a second order correction for each image pixel from the temperature difference and sum. The method is limited to areas of low topographic slope--probably 20 degrees or less--and is most applicable to HCMM data that have a 500-m resolution and can be merged with the DMA digital terrain data. The technique is applicable to aircraft data, exclusive of areas with rugged relief, but requires digital terrain data at appropriately higher resolution and is thus not generally available.

Acknowledgment

This research was supported in part under NASA contract S-40256-B.

Figure 1.--The azimuth variation of the topographic correction factor is plotted versus azimuth for the temperature day and night and temperature difference at two latitudes (30° and 50°), assuming a value of $h/W_1 = 138$ (using $\varepsilon = 1$, $\overline{v}_0 = 280$ K, P = 1500). Appendix One: Fourier coefficients for the topographic slope effect.

Let
$$f(t) = \sum_{k=0}^{r} B_k \cos (\omega kt - \theta_k)$$
 (1)
where $f(t) = \langle \cos z_d \rangle - \langle \cos z_0 \rangle$
 $\langle \cos z_d \rangle = \cos z_d \quad t_{gg} \langle t \langle t_{gg} \rangle$
 $= 0 \quad otherwise$
 $\langle \cos z_0 \rangle = \cos z \quad -t_1 \langle t \langle t_1 \rangle$
 $= 0 \quad otherwise$
 $\cos z_d = A \cos \omega t + B \sin \omega t + C$
 $\cos z = \cos \lambda \cos \delta \cos \omega t + \sin \lambda \sin \delta$
 $A = \cos d \cosh cos \delta - \sinh d \cosh cos \delta \sin \lambda$
 $B = \sinh \sin \phi \cos \delta$
 $C = \cosh \sinh \sinh \delta + \sinh \cosh cos \delta$
(Watson, 1975;1979)

$$\omega t_1 = \pi/2 + \sin^{-1}(\tan\lambda \ \tan\delta)$$

$$\omega t_{SS} = \pi/2 + MIN(\sin^{-1}(\tan\lambda \ \tan\delta), \ \sin^{-1}(C/R) + \tan^{-1}(D/A))$$

$$\omega t_{ST} = -\pi/2 + MAX(-\sin^{-1}(\tan\lambda \ \tan\delta), \ -\sin^{-1}(C/R) + \tan^{-1}(B/A))$$

and $R = \sqrt{A^2 + B^2}$

Because the solar declination is a small angle, $|\delta| < 23.5^{\circ}$ and the topographic slopes are assumed to be small $|d| < 20^{\circ}$ we shall introduce the small angle approximations for both δ and d:

```
sin x \neq x

cos x = 1

x^2 = 0.
```

$$A = \cos \lambda - d \cos \phi \sin \lambda$$

$$B = d \sin \phi$$

$$C = \phi \sin \lambda$$

$$\omega t_1 = \pi/2 + \delta \tan \lambda$$

$$\omega t_{ss} = \omega t_1 + MIN (0, d \sin \phi/\cos \lambda)$$

$$\omega t_{sr} = -\omega t_1 + MAX (0, d \sin \phi/\cos \lambda)$$

From equation 1 and using the standard Fourier coefficient method

$$B_{k} \cos\theta_{k} \int_{-T/2}^{T/2} \cos^{2} \omega kt \, dt = 2 \frac{B_{k} \cos\theta_{k}}{\omega} \int_{0}^{\pi} \cos^{2} kx \, dx$$

$$= \int_{sr}^{t} \cos z \cos \omega kt \, dt = \int_{-t_{1}}^{t_{1}} \cos z \cos \omega kt \, dt$$

$$= \frac{A}{\omega} \int_{\omega t}^{\omega t} \cos x \cos kx \, dx = \frac{\cos\lambda}{\omega} \int_{-\omega t_{1}}^{\omega t_{1}} \cos x \cos kx \, dx$$

$$+ \frac{B}{\omega} \int_{\omega t}^{\omega t} \sin x \cos kx \, dx + \frac{C}{\omega} \int_{\omega t}^{\omega t} \cos kx \, dx - \sin\lambda \cdot \delta \int_{-\omega t_{1}}^{\omega t_{1}} \cos kx \, dx$$

$$= \frac{2d \cos\phi \sin\lambda}{\omega} \int_{0}^{\pi/2} \cos x \cos kx \, dx$$

In a similar fashion

$$\frac{2B_k \sin\theta_k}{\omega} \int_0^{\pi} \sin^2 kx \, dx = \frac{2d \sin\phi}{\omega} \int_0^{\pi/2} \sin x \sin kx \, dx$$

Thus

_'

Now
$$\int_{0}^{\pi/2} \cos x \cos kx \, dx = 1$$
 $k = 0$
 $= \pi/4$ $k = 1$
 $= 0$ $k = 3, 5, ...$
 $= (-1)^{T+1} / [(2T)^2 - 1]$ $k = 2T, T = 1, 2, ...$
and $\int_{0}^{\pi/2} \sin x \sin kx \, dx = 0$ $k = 0$
 $= \pi/4$ $k = 1$
 $= 0$ $k = 3, 5, ...$
 $= 2T(-1)^{T+1} / [(2T)^2 - 1]$ $k = 2T, T = 1, 2, ...$
Therefore
 $B_0 = -d \cos\phi \sin\lambda/\pi$
 $\theta_0 = 0$
 $B_1 = (d/2) \sqrt{\sin^2 \phi + \cos^2 \phi \sin^2 \lambda}$
 $\theta_1 = \tan^{-1} (-\tan \phi/\sin\lambda)$
 $B_{2T} = \frac{2d (-1)^{T+1}}{\pi [(2T)^2 - 1]} \sqrt{(2T \sin\phi)^2 + (\sin\lambda \cos\phi)^2}$
 $\theta_{2T} = \tan^{-1} (-2T \tan\phi/\sin\lambda)$
 $B_{2T+1} = 0$ $r = 1, 2, 3, ...$

۴.

References

- Cannon, P. L., 1973, The application of radar and infrared imagery to quantitative geomorphic investigations: Proc. of Remote Sensing of Earth Res. Second Annual Conf., Tallahoma, Tenn., p. 503-526, The Univ. of Tenn. Space Inst., Tullahoma.
- Carslaw, H. S., and Jaeger, J. E., 1959, Conduction of heat in solids: Oxford at the Clarendon Press, Second Edition, 510 p.
- Gillespie, A. R., and Kahle, A. B., 1977, Construction and interpretation of a digital thermal inertia image: Photogrammetric Eng. and Remote Sensing, v. 43, p. 983-1000.
- Hummer-Miller, Susanne, 981, Simple expressions for the diurnal variation of four atmospheric parameters for use in surface temperature models: Submitted to Journal of Geophysical Research.
- Miller, S. H., and Watson, Kenneth, 1977, Evaluation of algorithms for geological thermal-inertia mapping: Proceedings 11th International Symposium Remote Sensing of Environment, v. 2, p. 1147-1160.
- Offield, T. W., 1975, Thermal-infrared images as a basis for structure mapping, front range and adjacent plains in Colorado: Geological Society of America Bulletin, v. 86, p. 495-502.
- Pohn, H. A., Offield, T. W., and Watson, Kenneth, 1974, Thermal-inertia mapping from satellite discrimination of geologic units in Oman: U.S. Geological Survey Journal of Research 2, no. 2, p. 147-158.
- Pratt, D. A., and Ellyett, C. D., 1979, The thermal inertia approach to mapping of soil moisture and geology: Remote Sensing Env. 8, p. 151-168.

- Price, J. C., 1977, Thermal inertia mapping: A new view of the Earth: Journal Geophysical Res. 82, p. 2582-2590.
- Rowan, L. C., Offield, T. W., Watson, Kenneth, Cannon, P. J., and Watson, R. D., 1970, Thermal infrared investigations, Arbuckle Mountains, Oklahoma: Geological Society of America Bulletin, v. 81, p. 3549-3562.
- Sabins, F., 1969, Thermal infrared imagery and its application to structural mapping in Southern California: Geological Society of America Bulletin, v. 80, p. 397-404.
- Schneider, S. R., McGinnis, D. F., Jr., and Pritchard, J. A., 1979, Use of satellite infrared data for geomophology studies: Remote Sensing Environment, v. 8, p. 313-330.
- Watson, Kenneth, 1970, A. Introduction and summary, B. Data analysis techniques, Part 1, Remote sensor application studies progress report, 1968-69: Clearing house for Fed. Sci. and Tech. Info (CFSTI), Doc. PB-197-098.
- Watson, Kenneth, 1971, A computer program of thermal modeling for interpretabion of infrared images: NTIS PB-203-578.
- Watson, Kenneth, 1975, Geologic applications of thermal infrared images: Proceedings IEEE 63, no. 1, p. 128-137.
- Watson, Kenneth, 1979, Thermal phenomena and energy exchange in the environment, in Mathematical and Physical Principles of Remote Sensing: Centre National D'Etudes Spatiales, Toulouse, France, p. 104-174.
- Watson, Kenneth, Rowan, L. C., and Offield, T. W., 1971, Applications of thermal modeling in the geologic interpretation of IR images: Proceedings Seventh International Symposium Remote Sensing of Environment, Ann Arbor, Michigan, v. 3, 7= 2017-2041.

Wolfe, E. W., 1971, Thermal IR for geology: Photogrammetric Eng., v. 37, p. 43-52.

ь † 5

e!

.

• *